iForest
Biogeosciences and Forestry

Research Article
doi: 10.3832/ifor4643-018
vol. 18, pp. 212-222

Kinetic, morphophysiological, and biochemical parameters as a strategy to select clones of *Eucalyptus* spp. more efficient in phosphorus uptake

Marcos Vinícius Miranda Aguilar [(1)], **Álvaro Luís Pasquetti Berghetti** [(1)], **Caroline Castro Kuinchtner** [(1)], **Thomas Wink Peixoto** [(2)], **Matheus S de Souza Kulmann** [(1)], **Daniel Vinicios Valsoler** [(2)], **Tais Dorneles de Azevedo** [(2)], **Vanessa Marques Soares** [(3)], **Gustavo Brunetto** [(3)], **Luciane Almeri Tabaldi** [(2)]

Eucalyptus **clones are typically selected based on their rooting capacity, wood quality, and resistance to drought, frost, and disease. However, kinetic, morphophysiological, and biochemical parameters that determine the uptake efficiency of nutrients such as phosphorus (P) are often not considered in breeding programs. This study aimed to select *Eucalyptus* clones based on P uptake efficiency using kinetic, morphophysiological, and biochemical parameters. The experiment was set up in a 2 × 3 factorial arrangement, the first factor being P levels: 16.5 mg P L^{-1} (high P) and 4.65 mg P L^{-1} (low P) in half-strength Hoagland's nutrient solution, and the second factor being three *Eucalyptus* spp. clones (*E. saligna*, *E. urograndis*, and *E. dunnii*), with six replications per treatment. Kinetic parameters (V_{max}, K_m, C_{min} and I), as well as morphological parameters in shoots and roots, biomass production, P concentrations in tissues, photosynthetic parameters, chlorophyll *a* fluorescence, photosynthetic pigments, metabolic enzyme activity and oxidative stress were evaluated. *Eucalyptus saligna* showed the highest P influx rates and the lowest values of C_{min}, while *E. urograndis* presented the lowest values of K_m under low P supply. Both *E. saligna* and *E. urograndis* resulted more efficient at phosphorus uptake, indicating P absorption efficiency at low concentrations. *Eucalyptus dunnii* showed the highest values of K_m and C_{min} for P, indicating adaptation to environments with greater P availability. Thus, P kinetic parameters could be used in *Eucalyptus* selection and breeding programs, as they assist in predicting P uptake in environments with different concentrations of this nutrient.**

Keywords: Eucalypts Clones, Maximum Uptake Rate (V_{max}), Michaelis-Menten Constant (Km), Minimum Concentration (C_{min}), P Uptake Efficiency

Introduction

Eucalyptus is the most widely planted genus of hardwood trees around the world (Scanavacca Júnior & Garcia 2021), consisting of about 700 species native to Australia and Indonesia, along with several hybrids developed to exploit different plant characteristics. Fast growth and adaptability to a wide range of tropical and subtropical regions, combined with the versatile properties of wood for energy, lamination, sawmilling, paper, and cellulose, ensure its prominent position in the current forestry landscape (Lima et al. 2019).

Eucalyptus saligna Smith, *Eucalyptus dunnii* Maiden, and the hybrid *E. urograndis* are clones grown in forest stands around the world. Both *E. dunnii* and *E. saligna* are economically important due to their tolerance to cold and frost, fast growth, and high-quality wood (Kulmann et al. 2021). *Eucalyptus urograndis* adapts well to various environmental conditions, exhibiting excellent productivity rates and desirable wood characteristics for multiple industrial purposes (Manca et al. 2020).

Eucalyptus clones used in commercial plantations are usually selected based on wood quality, productivity, rooting capacity, tolerance to drought, cold, frost, pests, and diseases (Kulmann et al. 2021). However, *Eucalyptus* trees are typically grown in soils with low natural fertility and high phosphorus (P) adsorption capacity in functional groups of reactive soil particles, such as iron (Fe), aluminum (Al), and manganese (Mn) oxides (Meng et al. 2021). Therefore, applying phosphate fertilizers to soils is necessary to increase P availability, supplying the demand of plants such as the *Eucalyptus*. Currently, plant production is highly dependent on phosphate fertilizers. It is estimated that approximately 20 million tons of P per year are used worldwide, with a usage of less than 10% (Baligar & Fageria 2015).

For the above reason, it would be desirable to select or develop nutritionally efficient genotypes that can grow and produce even in soils with low fertility (Paula et al. 2022, Silva et al. 2023). This approach would decrease the amount of P required in the field, cut down on production costs and reduce the potential risk of soil and

(1) Forest Sciences Department, Federal University of Santa Maria, Av. Roraima no. 1000 Cidade Universitária Bairro - Camobi, Santa Maria - RS, 97105-900 (Brazil); (2) Biology Department, Federal University of Santa Maria, Av. Roraima no. 1000 Cidade Universitária Bairro - Camobi, Santa Maria - RS, 97105-900 (Brazil); (3) Soil Science Department, Federal University of Santa Maria, Av. Roraima no. 1000 Cidade Universitária Bairro - Camobi, Santa Maria - RS, 97105-900 (Brazil)

@ Marcos Vinícius Miranda Aguilar (aguilarmarcos2009@hotmail.com)

Received: May 20, 2024 - Accepted: Mar 31, 2025

Citation: Miranda Aguilar MV, Pasquetti Berghetti ÁL, Kuinchtner CC, Wink Peixoto T, De Souza Kulmann MS, Valsoler DV, Dorneles De Azevedo T, Marques Soares V, Brunetto G, Almeri Tabaldi L (2025). Kinetic, morphophysiological, and biochemical parameters as a strategy to select clones of *Eucalyptus* spp. more efficient in phosphorus uptake. iForest 18: 212-222. - doi: 10.3832/ifor4643-018 [online 2025-08-08]

Communicated by: Pierluigi Paris

water contamination. Moreover, P reserves in the world are limited, and it is estimated that the deposit of phosphate rocks will be depleted in just 50 years (Antunes et al. 2022). To this end, the use of genotypes with greater capacity for nutrient uptake may be a viable strategy to enhance the efficiency of fertilizers, allowing a reduction in the doses currently used. Thus, using kinetic patterns of nutrient uptake as criteria for selecting genotypes may be a key method to maximize nutritional efficiency in plantations. Furthermore, such research could help identify genotypes capable of producing in areas with low soil fertility.

Kinetic parameters related to the uptake efficiency of nutrients, such as P, are traditionally not considered in the selection of *Eucalyptus* clones, though P is the primary nutrient that affects the growth and development of this species. This is because P within the plant is a key component in the synthesis of nucleic acids, proteins, hormones, adenosine monophosphate, activation and deactivation of enzymes, redox reactions, and carbohydrate metabolism (Brunetto et al. 2019).

The kinetic parameters of nutrient uptake are represented by the maximum uptake rate (V_{max}), Michaelis-Menten constant (K_m), minimum concentration (C_{min}), and influx rate (I) (Martinez et al. 2015). Such parameters allow us to predict greater or lesser efficiency of ion (*e.g.*, phosphate) uptake by plant roots at a given concentration in the medium (Batista et al. 2016). V_{max} represents the maximum uptake rate of the membrane transporters (Fernandes et al. 2022), and I refers to the flow or the rate of ion uptake in a solution with a specific concentration (C). Therefore, C refers to the concentration of the ion of interest present in solution at the time of collection (Paula et al. 2022). The constant C_{min} is the minimum ion concentration in the kinetic period, and K_m refers to the affinity coefficient of the transporter for solute (Fernandes et al. 2022).

In addition to these parameters, analyzing the morphological characteristics of the root system allows us to correlate the depletion of P forms in the solution with the genetic characteristics of the plant. This is because changes in root morphological characteristics may indicate which plants are better adapted to environments with low nutrient availability (Bulgarelli et al. 2019, Jin et al. 2024). Physiological and biochemical characteristics can also be important parameters in determining nutritional efficiency, as biomass production and plant growth are directly related to photosynthetic rates, pigment content, and antioxidant defense capacity (Zheng et al. 2022).

Kinetic parameters can help to identify plants that are better adapted to different edaphoclimatic conditions (Kulmann et al. 2020). It is expected that *Eucalyptus* clones have different phosphate uptake capacities and this will reflect on nutrient uptake and use efficiency, and consequently on morphophysiological and biochemical responses during growth and production. As a result, the ideal *Eucalyptus* clone would be one with high I and V_{max} as well as low C_{min} and K_m.

This study aimed to select *Eucalyptus* clones based on P uptake efficiency using kinetic, morphophysiological and biochemical parameters. Our results may contribute to the selection of *Eucalyptus* clones with higher nutrient uptake efficiency and to identifying those better adapted to the edaphoclimatic conditions of each region, increasing productivity and reducing fertilization costs.

Material and methods

Study area and plant material

The experiment was conducted in a greenhouse at the Department of Soils of the Federal University of Santa Maria (UFSM), Santa Maria, Rio Grande do Sul, southern Brazil (29° 43′ 07″ S, 53° 42′ 29.5″ W). The average temperature inside the greenhouse was 25 °C, and the relative humidity was approximately 60%.

The *Eucalyptus* spp. (*E. saligna, E. urograndis* and *E. dunnii*) clones used in this study were provided by the CMPC (Celulose Riograndense) company. The rooted minicuttings were produced through vegetative propagation in a clonal minigarden system, following the methodology employed by the company itself. Shortly after collection, the minicuttings were subjected to rooting in the greenhouse. The minicuttings were 12-cm long with two upper buds. The leaves had their leaf area reduced by 50% to preserve the photosynthetic area and reduce transpiration. The rooted minicuttings were cultivated in 55-cm³ polypropylene tubes. The substrate used for rooted minicuttings production was Carolina Soil®, composed of peat, *Sphagnum* spp., and vermiculite with the addition of 30% carbonized rice husk. Base fertilization was carried out with Osmocote®, a six-month controlled release fertilizer (CRF) composed of 15% N; 9% P_2O5; 12% KCl; 1% Mg, 2.3% S; 0.05% Cu; 0.06% Mn; 0.45% Fe, and 0.2% Mo.

The initial characterization of six plants from each *Eucalyptus* clone was conducted (Tab. 1) on the ninetieth day after rooting. The remaining rooted minicuttings were kept in a greenhouse for seven days to acclimatize. During this period, the rooted minicuttings were irrigated every day until the experiment was set up.

Experimental design

The *Eucalyptus* rooted minicuttings were removed from the tubes, and the roots were carefully washed to remove the surrounding substrate 98 days after rooting. The roots were then immersed in pots containing 6 L of full-strength Hoagland's nutrient solution, where they remained for seven days until this first step of acclimatization was complete. The full-strength nutrient solution contained (in mg L^{-1}) NO_3^- =196; NH_4^+ = 14; P = 31; K = 234; Ca = 160; Mg = 48.6; S = 70; Fe-EDTA = 5; Cu = 0.02; Zn = 0.15; Mn = 0.5; B = 0.5; and Mo = 0.01.

A sheet of Styrofoam with a hole in the middle was placed on top of each pot, allowing the plant to grow through it. The styrofoam sheet helped plant fixation and reduce evaporation of the solution in each pot. Aeration of the solution in each container was done via PVC microtubes connected to an air compressor. The microtubes were inserted into the solution through the styrofoam sheet in each pot.

The experiment was set up in a completely randomized design. A 2 × 3 factorial scheme was adopted, with the first factor being P levels: 16.5 mg P L^{-1} (high P) and 4.65 mg P L^{-1} (low P) in half-strength Hoagland's nutrient solution, and the second factor being three clones of *Eucalyptus* spp. (*E. saligna, E. urograndis* and *E. dunnii*) with six replications per treatment, totaling 36 experimental units. Each replication

Tab. 1 - Morpho-physiological characterization of *Eucalyptus* clones 90 days after rooting. (SDW): Shoot dry weight (g plant^{-1}); (RDW): root dry weight (g plant^{-1}); (H): height (cm); (DC): stem diameter (mm); (NF): number of leaves; (Leaf A): leaf area (cm^2); (Fv/Fm): maximum quantum yield of PSII.

Clones	SDW (g plant^{-1})	RDW (g plant^{-1})	H (cm)	DC (mm)	NF	Leaf A (cm^2)	Fv/Fm
E. saligna	1.08 ± 0.01	0.42 ± 0.04	24.5 ± 1.4	2.65 ± 0.46	7 ± 1.4	115 ± 7	0.794 ± 0.01
E. urograndis	1.12 ± 0.03	0.47 ± 0.01	26.5 ± 2.5	3.85 ± 0.61	11 ± 1.3	120 ± 8	0.735 ± 0.02
E. dunnii	1.13 ± 0.01	0.38 ± 0.01	27.1 ± 3.3	2.96 ± 0.41	19 ± 4.5	110 ± 4	0.770 ± 0.01

consisted of one plant per pot. The P concentrations and the strength levels of the elements present in the nutrient solution were determined through preliminary tests and previous experiments conducted in our laboratory, after reviewing scientific literature and adapting protocols used by the GEPACES research group (Paula et al. 2018, 2022, Kulmann et al. 2020).

After seven days of acclimatization in full-strength nutrient solution, the two levels of P (high and low) were added in half-strength nutrient solution, where plants remained for additional 21 days, completing the second acclimatization period. During this period, the solution was renewed every five days and the pH was adjusted to 6.0 ± 0.2 every two days by adding 1 mol L^{-1} HCl or 1 mol L^{-1} NaOH.

After the periods of acclimatization, the clones were induced to deplete nutrient reserves in a 0.03 mol L^{-1} calcium sulfate ($CaSO_4$) solution for 30 days, totaling 58 days of cultivation in a hydroponic system. This solution was used to maintain the electrochemical potential of cell membranes and preserve cell wall integrity (Paula et al. 2018).

Kinetics of net phosphate uptake

After 30 days of depletion of nutrient reserves in $CaSO_4$ (0.03 mol L^{-1}), the clones were transferred to a half-strength Hoagland's nutrient solution containing 16.5 mg P L^{-1} (high P) and 4.65 mg P L^{-1} (low P) along with other nutrients. The clones were kept under these conditions for one hour to simulate plant growth in the soil, which constantly absorb nutrients, following the kinetic model suggested by Claassen & Barber (1974). The solution was subsequently replaced, maintaining two levels of P and the same nutrient concentration as half-strength Hoagland's solution, for the collection of aliquots of the solution itself.

The solution was collected for a 72-h period. Fifteen milliliters of solution from each container were collected at time zero (0), when the half-strength Hoagland's solution was replaced. Then, 15 mL aliquots were collected every six hours during the first 24 hours (0; 6; 12; 18; 24h), every three hours between 24 and 48 hours, and every hour between 48 and 72 hours. The solutions were then frozen at -10 °C and stored for subsequent P analysis. The phosphorus content of the solution aliquots collected during the 72-h period was determined by colorimetry using a UV-visible spectrophotometer (SF325NM, Bel Engineering, Italy), according to the methodology described by Murphy & Riley (1962).

The kinetic parameters (V_{max} and K_m) were calculated according to P concentrations in the solution, initial and final solution volumes in pots, and root weight values using the Influxo software. The C_{min} was determined based on P concentrations in the nutrient solution during the 72-h evaluation period. Influx rate (I) was calculated (eqn. 1) according to Michaelis-Menten and modified by Nielsen & Barber (1978):

$$I = \left[\frac{V_{max} \cdot (C - C_{min})}{K_m + (C - C_{min})} \right] \quad (1)$$

where V_{max} is the maximum uptake rate of membrane transporters, C is the concentration in solution at the time of collection, C_{min} is the minimum concentration over the 72 hours, and K_m is the coefficient of transporter affinity for solute.

Photosynthetic parameters

After 56 days of cultivation in the hydroponic system, during the period of depletion of internal reserves, we analyzed the physiological parameters of the photosynthetic apparatus of each plant. These analyses took place from 8:00 am to 10:30 am with an infrared gas analyzer (IRGA, Infrared gas analyzer, Mod. Li-COR® 6400 XT). During this time, photosynthetic rate (A), transpiration rate (E), intercellular CO_2 concentration (C_i), and water use efficiency (WUE) were determined at an ambient CO_2 concentration of 400 µmol mol^{-1} at 20-25 °C, 50 ± 5% relative humidity and photon flux density of 1500 µmol m^{-2} s^{-1}.

Chlorophyll a fluorescence

Chlorophyll *a* fluorescence was also determined after 56 days of cultivation using a portable light-modulated fluorometer (Junior-Pam Chlorophyll Fluorometer, Walz Mess-und-Regeltechnik, Germany). Measurements were taken from fully expanded leaves of each plant on a sunny day between 8:00 am and 10:30 am. Before these measurements, the leaves were dark-adapted for 30 min to determine initial fluorescence (Fo). Subsequently, the leaves were subjected to a saturating light pulse (10,000 µmol m^{-2} s^{-1}) for 0.6 s to determine maximum fluorescence (Fm). The electron transport rate (ETRm) was determined from the fluorescence induction curve (1,500 mmol m^{-2} s^{-1}). Lastly, the maximum quantum yield of PSII (Fv/Fm) was calculated as the ratio between variable fluorescence (Fv = Fm- Fo) and maximum fluorescence.

Morphological parameters

Three plants from each treatment were collected for growth analysis, totaling 18 plants. Before the experiment's installation and at its conclusion, the shoot height and main root length of the plants were measured using a millimeter ruler. Based on these measurements, we calculated root increase (R_I – eqn. 2) and height increase (H_I – eqn. 3)

$$R_I = L_{fin} - L_{init} \quad (2)$$

$$H_I = H_{fin} - H_{init} \quad (3)$$

where L_{init} and L_{fin} are the initial and final length of the main root, respectively, while H_{init} and H_{fin} are the initial and final height of the plants, respectively.

After evaluating the kinetic period of 72 hours, plants were removed from the nutrient solution, separated into shoots and roots and the remaining solution in each pot was measured. Leaf area was determined using WinRhizo Pro® 2013 software (Regent Instrument Inc., Canada) coupled to an EPSON Expression 11000® scanner equipped with additional light (TPU) and a resolution of 200 dpi. The leaf area of each plant was calculated (cm^2 $plant^{-1}$) from the digitized images. Morphological characterization of the root system was performed using images scanned with WinRhizo Pro 2013 software, coupled to an EPSON Expression 11000 scanner, at a resolution of 600 dpi. Digitized images were used to determine values for total root length (cm $plant^{-1}$), root surface area (cm^2 $plant^{-1}$), root volume (cm^3 $plant^{-1}$), and average root diameter (mm).

The leaves and roots were then dried in a forced air circulation oven (65 ± 1 °C) until constant weight was reached. Subsequently, the samples were weighed on a precision digital scale (0.0001 g) to determine shoot dry weight (SDW), root dry weight (RDW), and total dry weight (TDW = SDW + RDW).

Tissue P analysis

Immediately after weighing, the dry mass of shoots and roots was ground in a Wiley mill and the tissue was passed through a 2 mm sieve. It was then submitted to nitro-perchloric digestion (EMBRAPA 1999). The P content in the extract was determined by the method of Murphy & Riley (1962) in a UV-visible spectrophotometer (1105, Bel Photonics) at 880 nm. Phosphorus (P) accumulation in leaves, roots and the total plant was determined based on the P concentration in each organ and the respective biomass. For leaves and roots, the value was obtained by multiplying the P concentration by the corresponding dry biomass. Total P accumulation in the plant was calculated by the sum of the values obtained for leaves and roots.

The following efficiency indices for P were determined (Siddiqi & Glass 1981): P absorption efficiency (PAE – eqn. 4), P use efficiency in roots (Root PUE – eqn. 5), in shoots (Shoot PUE – eqn. 6) and the total P use efficiency (Total PUE – eqn. 7):

$$PAE = (P_{acc}\,\text{plants}) / (RDW)^{-1} \quad (4)$$

$$\text{Root } PUE = (RDW)^2 / (P_{acc}\,\text{roots})^{-1} \quad (5)$$

$$\text{Shoot } PUE = (SDW)^2 / (P_{acc}\,\text{shoots})^{-1} \quad (6)$$

$$\text{Total } PUE = (TDW)^2 / (TDW)^{-1} \quad (7)$$

where P_{acc} *plants* is the P accumulation in plants (µg), P_{acc} *roots* is the P accumulation in roots (µg); P_{acc} *shoots* is the P accumulation in shoots (µg), *RDW* is the root dry weight (mg), *SDW* is the shoot dry weight (mg), and *TDW* is the total dry weight (mg).

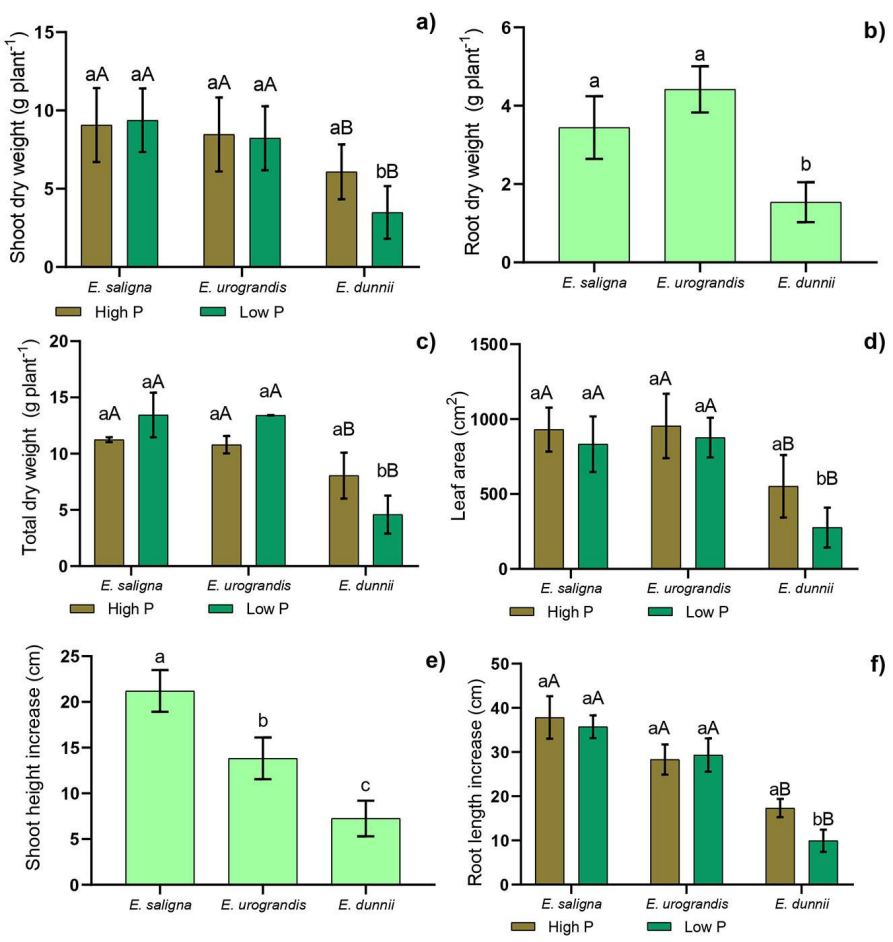

Fig. 1 - Mean values of (a) shoot dry weight (*SDW*), (b) root dry weight (*RDW*), (c) total dry weight (*TDW*), (d) leaf area, (e) shoot height increase (H_i), (f) and main root increase (R_i) in *Eucalyptus* clones grown in Hoagland's nutrient solution with low (green columns) and high (brown columns) P availability after 30 days of depletion of internal reserves. Means followed by lowercase letters differ ($p<0.05$) between P levels in the *Eucalyptus* clone after Student's *t*-test. Means followed by capital letters differ ($p<0.05$) between *Eucalyptus* clones within the P level after the Tukey test. Bars represent mean ± standard deviation.

Biochemical parameters

After evaluating the 72-h kinetic period, three plants from each treatment were also collected for biochemical analysis, totaling 18 plants. Fresh samples of leaves and roots were frozen (-80 °C) and subsequently macerated with liquid N to determine the biochemical parameters. Chlorophylls *a* and *b* and carotenoids were extracted according to the method of Hiscox & Israelstam (1979). Total chlorophyll was obtained by summing chlorophyll *a* and chlorophyll *b*. Guaiacol peroxidase (POD) activity was determined according to Zeraik et al. (2008) using guaiacol as substrate. Results were expressed in units of enzyme per mg of protein (U mg^{-1} protein). Superoxide dismutase (SOD) activity was determined using the spectrophotometric method described by Giannopolitis & Ries (1977). The unit of SOD was defined as the amount of enzyme that inhibits NBT photoreduction by 50% (Beauchamp & Fridovich 1971). Acid phosphatase activity was determined according to the method described by Tabaldi et al. (2007). The reaction was initiated by adding the substrate (PPi) at a final concentration of 3.0 mM and terminated by adding 200 µL of 10% trichloroacetic acid (TCA) to a final concentration of 5%. Inorganic phosphate (Pi) was quantified at 630 nm, using malachite green as a colorimetric reagent and KH_2PO_4 as a standard for the calibration curve. Hydrogen peroxide levels were determined according to Loreto & Velikova (2001) and expressed as µmol g^{-1} fresh weight. Lipid peroxidation levels were determined by the concentration of malondialdehyde (MDA), following the method by El-Moshaty et al. (1993) and expressed as nmol of MDA mg^{-1} of protein.

Statistical analysis

The results of the morphophysiological and biochemical parameters were subjected to homogeneity and normality tests. The data were then processed and analyzed using the R software (R Core Team 2019). When the effects of treatments were significant, the results of *I*, V_{max}, K_m, and C_{min} for each *Eucalyptus* clone were compared using the Tukey test ($p<0.05$). The difference in P concentrations over 72 hours for each clone was compared by Student's *t*-test ($p<0.05$).

To verify the effects of the treatments on the response parameters, we submitted the data to a multivariate analysis of principal components (PCA) using the "FactoExtra" package (Kassambara & Mundt 2017) and the R software (R Core Team 2019).

Results

Morphological parameters

A significant interaction ($p\leq0.05$) was observed between the factors (P levels × *Eucalyptus* clones) for shoot and total dry weight, leaf area, main root increase, and average root diameter. This indicates that the combination of the factors influenced the expression of these characteristics (Fig. 1 and Fig. S1d in Supplementary material).

When comparing P levels, we found that *E. saligna* and *E. urograndis* showed no significant differences for shoot and total dry weight, leaf area, and main root increase. Still, the lowest values for these parameters were found in *E. dunnii* under low P (Fig. 1a, Fig. 1c, Fig. 1d, Fig. 1f). Furthermore, we observed that the low P supply promoted a reduction in these parameters for *E. dunnii* (Fig. 1a, Fig. 1c, Fig. 1d, Fig. 1f).

There was no significant interaction among the clones within each P level for root dry weight, shoot height increase (Fig. 1b and Fig. 11e), root length, root surface area, and root volume (Fig S1a, Fig. S1b and Fig. S1c – see Supplementary material). The lowest values of root dry weight and shoot height increase were observed in *E. dunnii*, which was significantly different from the other clones under study (Fig. 1b, Fig. 1e). Higher values for root length, surface area, and volume were found in *E. urograndis* and *E. saligna* in comparison to *E. dunnii* (Fig S1a, Fig. S1b and Fig. S1c – see Supplementary material). Comparing the clones within each P level, we found that *E. dunnii* had the lowest average root diameter under high P (Fig. S1d).

Physiological parameters

A significant difference (p≤0.05) among the *Eucalyptus* clones was observed for photosynthetic rate (*A*), transpiration rate (*E*), intercellular CO_2 concentration (C_i), and water use efficiency (WUE) (Fig. S2 in Supplementary material). The lowest values of *A*, *E*, and C_i were found in *E. dunnii*, which was considerably different from the other clones (Fig. S2a, Fig. S2b, Fig. S2c). However, the highest water use efficiency (WUE) was found in *E. dunnii*, corresponding to increases of 42% and 61.55% compared to *E. urograndis* and *E. saligna*, respectively (Fig. S2d in Supplementary material).

When comparing the clones within each P level, we found that *E. dunnii* exhibited the highest values of initial fluorescence (*Fo*) and maximum fluorescence (*Fm*) under both high and low P, similar to *E. urograndis* under low P (Fig. 2a, Fig. 2b). When comparing the clones within each P treatment, we observed that *E. dunnii* showed the lowest values of electron transport rate (ETRm) under low and high P supply, but did not differ from *E. saligna* under high P and *E. urograndis* under low P (Fig. 2c). Also, the highest ETRm values were observed in *E. saligna* under low P and in *E. urograndis* under high P (Fig. 2c).

There was no significant interaction between *Eucalyptus* clones and P levels for maximum quantum yield of photosystem II (*Fv/Fm* – Fig. 2d). However, a reduction of 14.38% in *Fv/Fm* was observed *in E. dunnii* under low P, compared to this clone under high P (Fig. 2d). Low P supply also promoted a 13.25% increase in total chlorophyll for *E. saligna* and 13.14% for *E. urograndis*, while causing a 24.39% decrease in total chlorophyll for *E. dunnii* (Fig. 2e). Lastly, there was no significant difference between *Eucalyptus* clones and P levels for carotenoid content (Fig. 2f).

Biochemical parameters, tissue P, and kinetic parameters related to P uptake

There was a significant effect (p≤0.05) of the interaction between the factors (P levels × *Eucalyptus* clones) for the biochemical parameters (Fig. 3), except for root membrane lipid peroxidation (data not shown).

When comparing P treatments, *E. saligna* and *E. dunnii* showed higher superoxide dismutase (SOD) and peroxidase (POD) activity in shoots under low P (Fig. S3a, Fig. S3c – see Supplementary material). However, there was no significant difference between P levels for SOD and POD activity in shoots of *E. urograndis*.

On the other hand, there was a reduction in SOD and POD activity in roots of *E. urograndis* under low P (Fig. S3b, Fig. S3d). Low P supply increased acid phosphatase activity in shoots and roots of *E. dunnii* and in shoots of *E. urograndis* (Fig. S3e, Fig. S3f). However, there was a decrease in acid phosphatase activity in shoots of *E. saligna* under low P (Fig. S3e in Supplementary material).

E. saligna showed the highest APase activity in shoots and roots under high P. The lowest APase activity in roots was found in *E. urograndis* under low P, while *E. dunnii* showed the highest APase activity in roots under low P (Fig. S3e, Fig. S3f).

The highest level of hydrogen peroxide (H_2O_2) was found in shoots of *E. urograndis* under low P. Low P supply promoted a decrease in H_2O_2 in shoots and roots of *E. dunnii* and in roots of *E. urograndis* (Fig. 3a, Fig. 3b). Furthermore, the highest value of lipid peroxidation was observed in shoots of *E. dunnii* under low P (Fig. 3c). Hydrogen peroxide levels among clones within each P treatment were higher in shoots of *E. urograndis* and in roots of *E. saligna* under low P. Furthermore, the highest values of MDA in shoots were found in *E. dunnii* under low P (Fig. 3c), while higher values were observed in *E. urograndis* and *E. dunnii* under high P (Fig. 3c).

The lowest P accumulation values in shoots, roots, and total accumulation were found in *E. dunnii* (Fig. 3a, Fig. 3b, Fig. 3c). It also showed the lowest values of P absorption efficiency (PAE), P use efficiency in roots (PUE_{root}), in shoots (PUE_{shoot}), and total P use efficiency (PUE_{total} – Fig. S4 in Supplementary material). Furthermore, there was no significant interaction among the

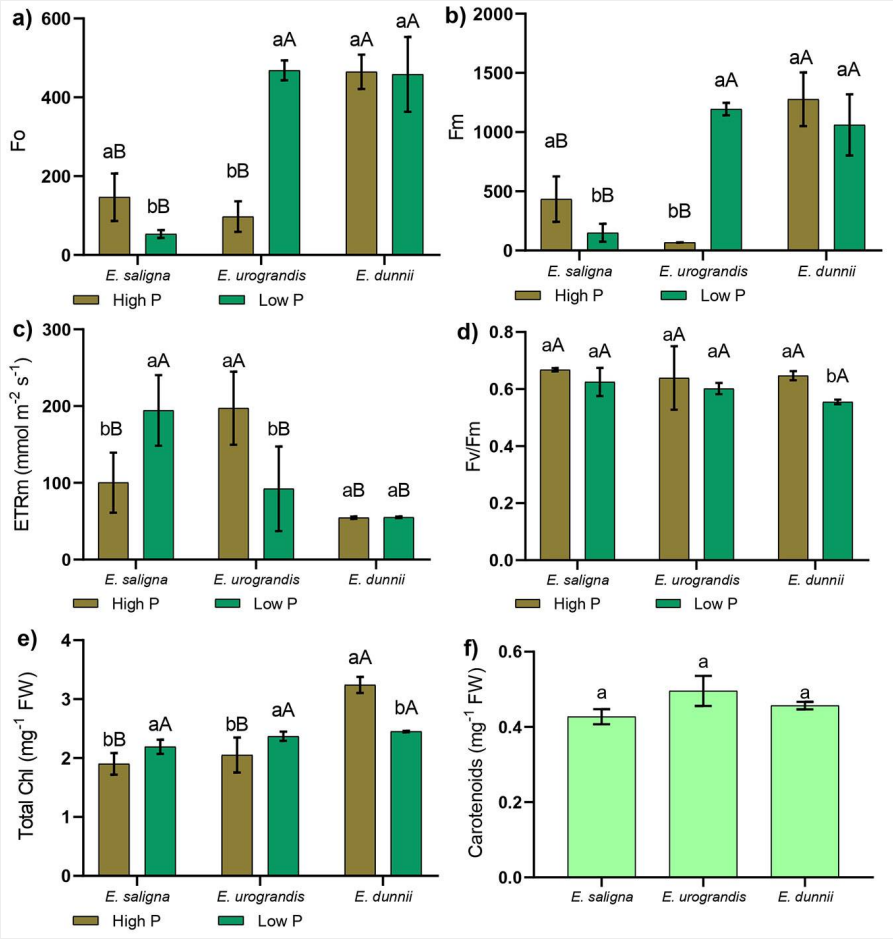

Fig. 2 - Mean values of (a) initial fluorescence (*Fo*), (b) maximum fluorescence (*Fm*), (c) electron transport rate (ETRm), (d) maximum quantum yield of PSII (*Fv/Fm*), (e) total chlorophyll, and (f) carotenoids in *Eucalyptus* clones grown in Hoagland's nutrient solution with low and high P availability after 30 days of depletion of internal reserves. Means followed by lowercase letters differ (p<0.05) between P levels in the *Eucalyptus* clone after Student's *t*-test. Means followed by capital letters differ (p<0.05) between *Eucalyptus* clones within the P level after Tukey test. Bars represent mean ± standard deviation.

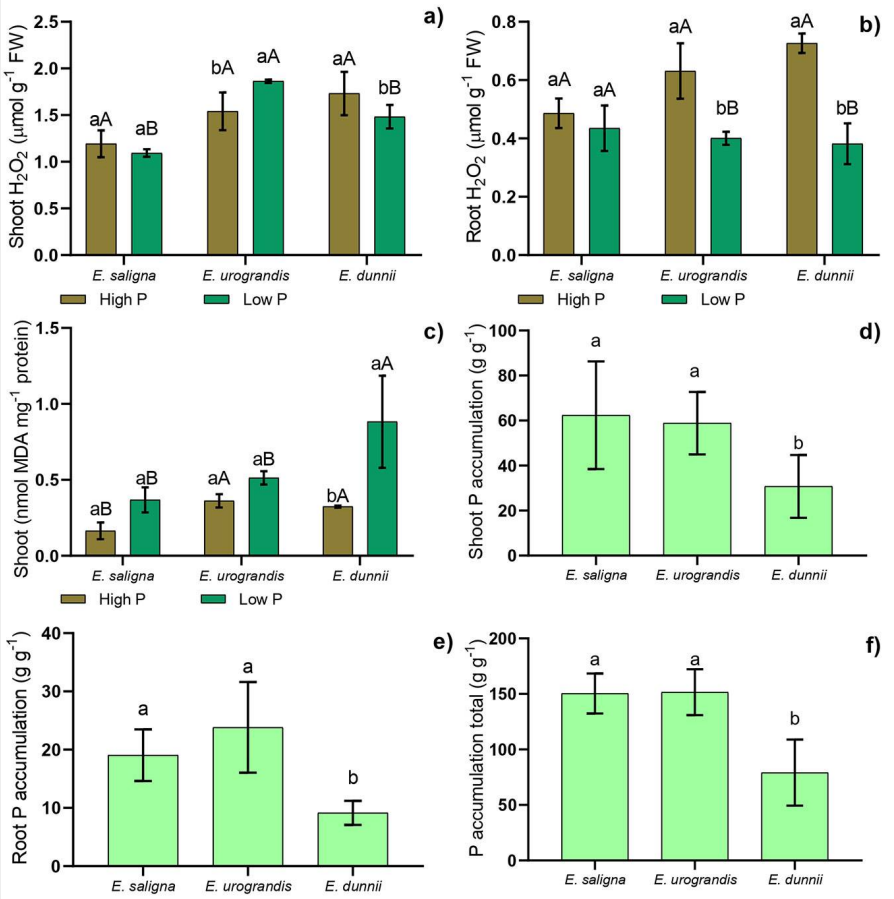

Fig. 3 - Mean values recorded for hydrogen peroxide (H_2O_2) concentration in shoots (a) and roots (b), membrane lipid peroxidation in shoots (c), P accumulation in shoots (d) and in roots (e) and total P accumulation (f) in *Eucalyptus* clones grown in Hoagland's nutrient solution with low and high P availability after 30 days of depletion of internal reserves. Means followed by lowercase letters significantly differ ($p<0.05$) between P levels within the *Eucalyptus* clone after Student's *t*-test. Means followed by capital letters significantly differ ($p<0.05$) between *Eucalyptus* clones within the same P level after Tukey test. Bars represent mean ± standard deviation.

clones within each P level for these parameters.

The comparison of clone performances within each P treatment revealed that *E. saligna* had the highest value of V_{max} under low P and *E. dunnii* showed the highest value of V_{max} under high P and low P (Fig. 4a). Furthermore, the highest values of K_m and C_{min} were found in *E. dunnii* under both P levels, while *E. urograndis* showed the highest C_{min} under low P (Fig. 4a).

The lowest V_{max} was observed in *E. dunnii* under low P (Fig. 4a). However, the highest C_{min} was found in *E. dunnii* under high P. The highest C_{min} in *E. urograndis* was observed under low P (Fig. 4a). Low P supply caused a decrease in V_{max} for *E. dunnii* (Fig. 4a). However, there was a reduction in K_m and C_{min} for *E. saligna* and *E. dunnii* under low P. Hence, differences in phosphate absorption among the clones were observed through phosphate uptake kinetics, as shown by the influx curve (Fig. 4a, Fig. 4b). *Eucalyptus saligna* initiated phosphate uptake even under low P concentration, resulting in lower C_{min} values compared to *E. dunnii* and *E. urograndis* (Fig. 4a, Fig. 4b).

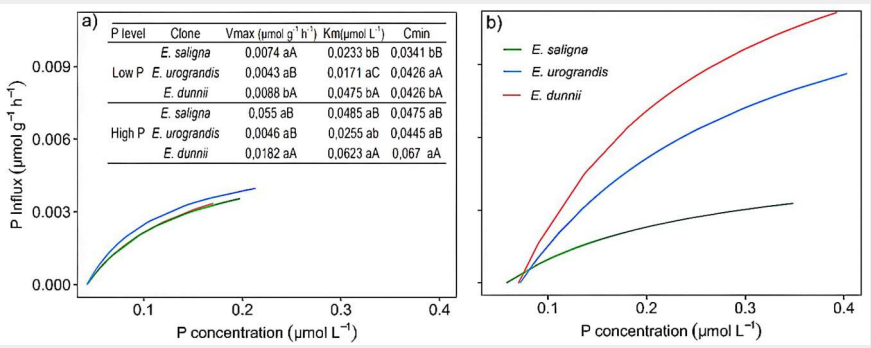

Fig. 4 - Influx rates and phosphate uptake kinetic parameters in *Eucalyptus* clones grown in Hoagland's nutrient solution with low (a) and high (b) P availability after 30 days of depletion of internal reserves. Means followed by lowercase letters are significantly different ($p<0.05$) between P levels in the *Eucalyptus* clone after Student's *t*-test. Means followed by capital letters significantly differ ($p<0.05$) between *Eucalyptus* clones within the P level after Tukey test.

Relationships among parameters

Principal component analysis (PCA) was performed based on the response parameters (Fig. 5). The sum of the first two components explained 57.6% of the data variability, with PC1 and PC2 accounting for 42.4% and 15.2%, respectively. PCA allowed us to analyze the behavior of *Eucalyptus* species under both P levels, revealing the existence of two groups: (i) *E. saligna* and *E. urograndis*; and (ii) *E. dunnii*. The first group (i) was primarily affected by the following response parameters: increase in shoot height (H_l), increase in main root (R_l), leaf area, total dry weight (*TDW*), shoot dry weight (*SDW*) and root dry weight (RDW), root surface area, root volume, root diameter, root length, P accumulation in shoots (Shoot P_{acc}), roots (Root P_{acc}) and total accumulation (*Total* P_{acc}), P aborption efficiency (PAE), P use efficiency in shoots (PUE_{shoot}), roots (PUE_{root}) and total use efficiency (PUE_{total}), net photosynthetic rate (*A*), intercellular CO_2 concentration (C_i), transpiration rate (*E*), electron transport rate (ETRm), maximum quantum yield of PSII (*Fv/Fm*), carotenoids (Carot), SOD in shoots (Shoot SOD) and in roots (Root SOD), and acid phosphatase in shoots (Shoot APase) and roots (Root APase). The second group (ii) was influenced by re-

sponse parameters: initial (Fo) and maximum fluorescence (Fm), hydrogen peroxide levels in shoots (Shoot H_2O_2) and in roots (Root H_2O_2), MDA concentration in shoots (Shoot TBARS), POD in shoots (Shoot POD) and in roots (Root POD), water use efficiency (WUE) and total chlorophyll (Total Chl).

Discussion

Morphological parameters

The studied clones of *E. saligna* and *E. urograndis* showed higher values of increase in height, dry matter production, leaf area, and P accumulation in shoots compared to *E. dunnii* (Fig. 1, Fig. S3d in Supplementary material), demonstrating different growth rates among the clones. This may have occurred due to the intense cell division and elongation that take place during vegetative growth, promoting an increase in dry matter, as well as the absorption and accumulation of nutrients such as P (Irfan et al. 2020). It is also noteworthy that the higher shoot dry matter production is an indication that plants had greater leaf area and, therefore, increased interception of sunlight, increasing C fixation, as well as total dry weight and height (Kulmann et al. 2021). These growth differences among *Eucalyptus* clones can also be confirmed in the field, since *E. saligna* and *E. urograndis* grow faster than *E. dunnii* in eucalyptus plantations.

The lowest values of shoot and root dry weight and the highest average root diameter in low P supply, along with a reduced P accumulation in shoot and root tissues, were observed in *E. dunnii* (Fig. 1, Fig. S1, fig. S3). This may be due to its lower efficiency in P uptake and use (Fig. S4), which reduces the translocation of P to growing organs, thereby resulting in reduced height and dry matter production (Li et al. 2022). On the other hand, higher values of root dry weight, length, surface area, and volume were found in *E. saligna* and *E. urograndis* in comparison to *E. dunnii*, resulting in increased P uptake (Fig. 1, Fig. S1, Fig. S3). This response occurs because larger root systems allow for exploring higher volumes of soil, thus increasing the probability of absorption of relatively immobile nutrients such as P (Pinto et al. 2020).

Nonetheless, the low supply of P led to an increase in the average root diameter of *E. dunnii* (Fig. S1d in Supplementary material). Root diameter expresses the volume of soil penetrated by the roots per unit of invested photosynthate. Thus, the roots of *E. dunnii* absorbed P less effectively (Fig. S4), as thick roots are shorter and therefore explore a smaller volume of soil per unit area of root surface, resulting in lower P uptake. This is because for every unit of biomass invested in the root, the development of thick roots provides less surface area in contact with the soil, compared to several thinner roots. Subsequently, this causes reduced growth and root dry matter production (Bernardino et al. 2019).

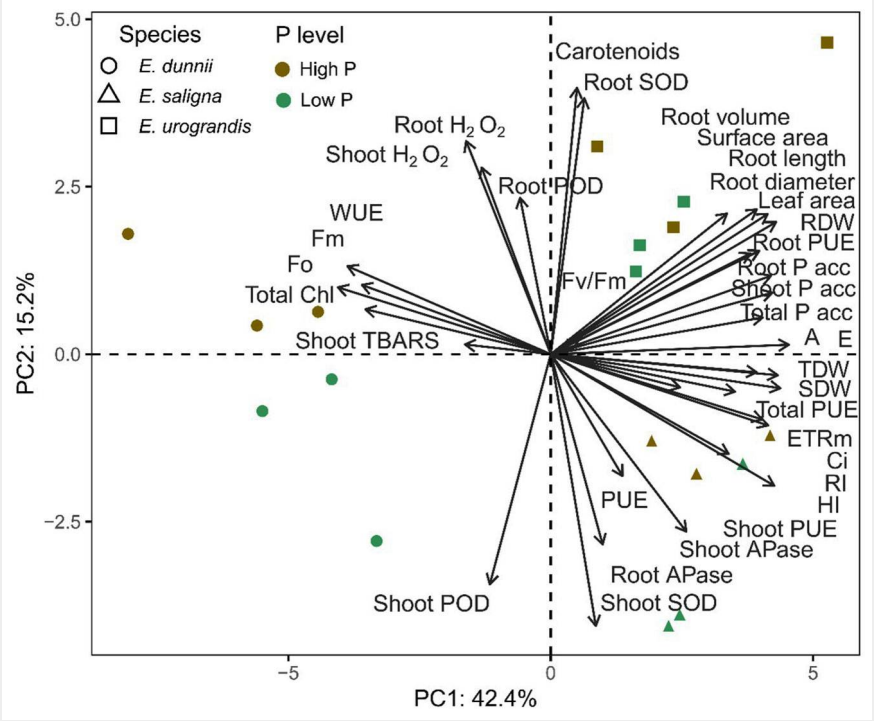

Fig. 5 - PCA biplot of the first two principal components (PC1, PC2) and the variable loadings on axes (arrows) in *Eucalyptus* clones grown in Hoagland nutrient solution with low and high P availability after 30 days of reduced internal nutrient reserves. Morphological parameters: height increase (HI), main root increase (RI), leaf area, total dry weight (TDW), shoot dry weight (SDW) and root dry weight (RDW). Root morphological parameters: root surface area, volume, diameter and length). Nutritional parameters: P accumulation in shoots (Shoot P acc), roots (Root P acc) and total P accumulation (Total P acc). Efficiency parameters: P absorption efficiency (PAE), P use efficiency in shoots (Shoot PUE), roots (Root PUE) and total P use efficiency (Total PUE). Physiological parameters: net photosynthetic rate (*A*), water use efficiency (WUE), intercellular CO_2 concentration (C_i), transpiration rate (*E*), electron transport rate (ETRm), maximum quantum yield of PSII (*Fv/Fm*), initial fluorescence (*Fo*) and maximum fluorescence (*Fm*), concentration of total chlorophyll (Total Chl), carotenoids (Carot), SOD in shoots (Shoot SOD) and roots (Root SOD), POD in shoots (Shoot POD) and roots (Root POD), hydrogen peroxide concentration in shoots (Shoot H_2O_2) and roots (Root H_2O_2), MDA concentration in shoots (Shoot TBARS) and acid phosphatase activity in shoots (Shoot APase) and roots (Root APase).

Kinetic parameters of P uptake

The clone *E. saligna* showed the highest rates of P influx and lower values of C_{min}, while *E. urograndis* presented the lowest values of K_m under low P supply (Fig. 4). The C_{min} results suggest that *E. saligna* has P transport proteins that are activated in lower P concentrations in the solution. In contrast, the low K_m values of *E. urograndis* indicate a high affinity for P at the absorption sites. The greater root length, surface area, and volume found in *E. saligna* (Fig. S1 in Supplementary material) may have contributed to the larger number of P transport proteins, resulting in increased P uptake efficiency (Li et al. 2022).

The lower C_{min} values suggest that *E. saligna* has a greater capacity for P uptake even in environments (solution or soil) with small concentrations of the nutrient, and it can access P through a higher number of absorption sites per root unit in different environments (Liu 2021) compared to *E. dunnii* (Fig. 4). Thus, *E. saligna* can be grown in solution or in soils with lower P availability. These results also make it possible to reduce the amount and frequency of phosphate fertilizer applications in *Eucalyptus* plantations cultivated with this clone, leading to decreasing phosphorus usage in the soil. This is also desirable because phosphate fertilizers are mainly produced from phosphate rock, a finite and non-renewable resource (Antunes et al. 2022).

Phosphate uptake kinetics highlighted clear differences in P uptake among the clones, as showed by the influx curve (Fig. 4b). The clone of *E. saligna* initiated P uptake in solution even under low concentrations, consequently resulting in lower C_{min} values compared to *E. dunnii* and *E. urograndis* (Fig. 4). This suggests that different *Eucalyptus* clones absorb P through different transport systems (Pereira et al. 2019). For instance, *E. saligna* possibly activates a

high-affinity system (HATS), while *E. dunnii* a low-affinity system (LATS), each mediated by more than one membrane protein with different enzyme kinetics (Yang et al. 2021). On the other hand, the lowest V_{max} values observed in *E. dunnii* (Fig. 4) suggest that it can activate a low-affinity P transport system, resulting in higher K_m and C_{min} (Pinto et al. 2020). Thus, the results showed that *Eucalyptus* clones differ in P uptake efficiency, based on the genetic characteristics of each clone.

The transport of P from the rhizosphere to the different plant tissues mainly involves multiple phosphate transporters (PHTs) belonging to subfamilies PHT1, PHT2, PHT3, or PHT4 located in the plasma membrane, plastid inner membrane, mitochondrial inner membrane, and Golgi compartment, respectively (Teng et al. 2017). Under stress conditions of P starvation, the PHT1 gene is strongly induced, increasing the root's ability to acquire P from soils and remobilize it within plants (Liu 2021). Studies conducted with rice (*Oryza sativa*) and *Arabidopsis thaliana* suggest that the PHT1 family genes play a role in remobilizing phosphorus (P) from senescent tissues and/or reserves to tissues in active development, and subsequently in plant development (Pereira et al. 2019). Phosphate transporters and transporter-like proteins function as phosphate sensors to regulate the expression of phosphate transporters, thereby maintaining phosphate homeostasis and optimizing nutrient and mineral utilization.

Physiological parameters

The higher values of photosynthetic rate found in *E. saligna* and *E. urograndis* clones differed significantly from those recorded in *E. dunnii* (Fig. S2a in Supplementary material). This is likely due to the increased transpiration rate in these clones, resulting in a greater water gradient between the solution and the plant, which stimulated P uptake and use efficiency, along with a higher leaf photosynthetic rate (Wang et al. 2018, Kulmann et al. 2021). However, the lower values of photosynthetic rates in *E. dunnii* possibly occurred because of lower P accumulation in shoots (Fig. S2a, Fig. 3c). Indeed, with low Pi availability in the stroma, photophosphorylation of ADP is impaired, resulting in a decrease in ATP synthesis and limited regeneration of ribulose 1,5-bisphosphate (RuBP – Hernández & Munné-Bosch 2015). The lowest transpiration rate values were also observed in the studied clones of *E. dunnii* (Fig. S2c). This may have occurred because plants with higher CO_2 levels in the leaf intercellular spaces close their stomata more frequently, reducing transpiration and increasing water use efficiency (WUE), as shown in our study (Fig. S2c, Fig. S2d). On the other hand, the lowest values found in *E. dunnii* contributed to reduced P uptake, resulting in a decrease in plant growth, as confirmed by the reduced height and lower dry matter production. Thus, the lowest values of photosynthetic parameters observed in *E. dunnii* (Fig. S2) possibly happened because of the low P accumulation in shoot tissues (Fig. 3d), which promotes changes in the composition of thylakoid membranes and photosynthetic pigments, or by the prevention of electron flow in the photochemical phase of photosynthesis (Ferreira et al. 2018).

The lowest values of initial fluorescence (*Fo*) and maximum fluorescence (*Fm*) in *E. saligna* under low P supply (Fig. 2a, Fig. 2b) demonstrated that plants showed little damage to the reaction center of photosystem II (PSII) and high excitation energy transfer from the light collecting system to the reaction center under this condition (Berghetti et al. 2020). With lower energy loss, the plants showed higher values of electron transport rate (ETRm) and growth (Fig. 2c, Fig. 1). This process occurs because energy dissipation leads to a decrease in fluorescence values, which in turn results in an increased formation of ATP and NADPH during the light reactions and carbon assimilation. Additionally, the higher *Fv/Fm* values in *E. saligna* and *E. urograndis* (Fig. 2d) also indicate that most light energy is utilized in the photochemical phase of photosynthesis, rather than being lost by chlorophyll *a* fluorescence (Kulmann et al. 2020). Thus, the increased growth and dry matter production in clones of *E. saligna and E. urograndis* corroborate the *Fv/Fm* results of PSII (Fig. 1, Fig. 2d).

On the other hand, the reduction in *Fv/Fm* found in the plants of *E. dunnii* under low P supply was due to the decrease in total chlorophylls in shoots (Fig. 2d, Fig. 2e). Lower pigment contents result in less absorption and light capture in different regions of the spectrum in the initial stages of the photosynthetic process (Janeeshma et al. 2022). As a result, there is a decrease in the transfer of resonance energy from the antenna complexes to the reaction centers, thereby reducing the amount of energy available for the photochemical reactions responsible for biomass production (Berghetti et al. 2020).

Carotenoid levels were not negatively influenced by P deficiency (Fig. 2f). This is noteworthy, as carotenoids not only function as antenna pigments for light absorption but also act as photoprotective pigments in the photosynthetic system. They protect chlorophyll by preventing the formation of singlet oxygen, a reactive oxygen species (ROS). They are non-enzymatic antioxidants suppressing ROS and free radicals (Meng et al. 2021).

Biochemical parameters and tissue P

Reactive oxygen species (ROS), such as H_2O_2 and $OH^{\bullet}$ and $O_2^{\bullet-}$ radicals, are naturally formed within cells, particularly in chloroplasts and mitochondria, as a result of electron transport and cellular respiration, respectively (Aguilar et al. 2023). However, ROS production is significantly increased under conditions of low P supply (Ferreira et al. 2018). The activation of the enzymatic antioxidant system in response to ROS formation is a common strategy employed by plants exposed to P deficiency (Brunetto et al. 2019). Superoxide dismutase (SOD) and guaiacol peroxidase (POD) are considered the main enzymes involved in eliminating ROS and maintaining homeostasis in plant cells (Alsherif et al. 2022).

We found *E. saligna* and *E. dunnii* showed higher SOD and POD activity in shoots under low P (Fig. S3a, Fig. S3c). The increase in SOD activity suggests its potential use in mitigating oxidative damage, as SOD converts the superoxide anion ($O_2^{\bullet-}$) into hydrogen peroxide (H_2O_2), which is often correlated with increased plant tolerance. Hydrogen peroxide is a ROS that, when accumulated at high levels in cells, can cause damage to cellular components or participate in reactions with the formation of ROS that are more harmful to cells (*e.g.*, hydroxyl radical – Mittler et al. 2022).

Guaiacol peroxidase participates in the conversion of H_2O_2 into water and oxygen through H_2O_2 dissociation, playing a crucial role in making plants tolerant to unfavorable conditions (Alsherif et al. 2022). The increase in POD activity in shoots of *E. saligna* and *E. dunnii* under lower P supply (Fig. S3c in Supplementary material) suggests that the ability to detoxify ROS is being upregulated, resulting in lower H_2O_2 values (Fig. 3). However, we observed that low P supply promoted a reduction in SOD in roots of *E. urograndis* (Fig. S3b). Consequently, low P supply did not influence the release of H_2O_2, and thus POD was also reduced, as the H_2O_2 levels were not high (Fig. 3, Fig. S3).

Even with the reduction of H_2O_2 levels in the *E. dunnii* clone, an increase in malondialdehyde (MDA) levels was observed in shoots (Fig. 3). This increase in membrane lipid peroxidation is related to the increase in other possible ROS produced by P stress, promoting an increase in MDA levels. Malondialdehyde is an oxidized product of membrane lipids and accumulates when plants are exposed to oxidative stress (Aguilar et al. 2023). Thus, the increase in MDA in *E. dunnii* under conditions of low P supply indicated oxidative stress in these plants (Fig. 3). As a result, it decreased P uptake and use efficiency, resulting in a lower photosynthetic rate and, consequently, a smaller increase in height and dry matter production.

There was no significant difference in lipid peroxidation levels in roots (data not shown). We found that the parameters related to oxidative stress were generally less affected in the roots than in the shoots. This can be attributed to the intense cell division and expansion of young leaves, which are metabolically more active, consequently demanding a greater amount of P. On the other hand, the roots had sufficient P to be utilized in respiration

and the maintenance of the antioxidant system in their tissues (Del-Saz et al. 2018).

In this study, we found that low supply of P promoted an increase in acid phosphatase (APase) in shoots and roots of *E. dunnii* (Fig. S3e, Fig. S3f in Supplementary material), likely due to lower tissue P accumulation (Fig. 3). Therefore, the increase in APase activity occurs to maintain the internal homeostasis of inorganic phosphate (Pi) to supply it from organic P compounds in the cytoplasm and vacuoles (Ferreira et al. 2018). This reflects the greater need for P remobilization through APase activity in shoots in response to the relatively low ability of the roots to acquire P and meet the demand of the shoots.

Higher values of tissue P accumulation, root PUE, shoot PUE and total PUE were found in *E. saligna* and *E. urograndis* (Fig. 3, Fig. S4). This response most likely occurred because the plant organs of these clones have different competitive abilities to accumulate P, which has a positive relationship with the formation of assimilates, thus promoting the acquisition of resources and the development of sink organs (Wang et al. 2018). This suggests that P accumulation in different organs is strongly linked to the formation of assimilates in these organs (Chen et al. 2020). However, the lower total P accumulation in *E. dunnii* can be credited to the remobilization of P from other storage tissues or organs to growing tissues (*e.g.*, leaves) or a consequence of lower P uptake efficiency.

Relationship among parameters

The results of principal component analysis (PCA) allowed us to clarify the effect of *Eucalyptus* species on phosphorus (P) levels in the soil. PCA revealed the existence of two groups based on response parameters : (i) *E. saligna* and *E. urograndis*; and (ii) *E. dunnii* (Fig. 5). There was a positive relationship of *E. saligna* and *E. urograndis* with growth parameters of the shoot and root system, P uptake efficiency, and status in the plant and photosynthetic efficiency. These *Eucalyptus* species have demonstrated higher P uptake efficiency, as well as improved shoot, root, and total P use efficiency, likely due to the better development of the root system (root surface area, volume, diameter and length), which facilitates soil exploration (Wang et al. 2018, Kulmann et al. 2021). This is supported by the positive correlation observed between shoot, root, and total phosphorus accumulation. With the increase of P in plant tissues, there was an improvement in leaf gas exchange conditions (*e.g.*, *A*, *E*, C_i, and WUE), as well as an increase in fluorescence efficiency (*e.g.*, ETRm and Fv/Fm – Kulmann et al. 2022). This led to an increased C fixation and assimilation in leaf tissues, resulting in an increase in shoot, root, and total dry matter production as well as leaf area, which contributed to the increase in height and main root length of *E. saligna* and *E. urograndis* (Berghetti et al. 2020, Kulmann et al. 2021).

The second group exhibited a positive relationship between *E. dunnii* and energy loss parameters, as indicated by fluorescence, oxidative stress, and antioxidant enzyme activity. This species exhibited sensitivity to stress conditions, particularly under low phosphorus (P) availability in the soil (Low P). Thus, there was an increase in the overproduction of ROS. *Eucalyptus dunnii* may have undergone an energy expenditure in response to the activation of both enzymatic and non-enzymatic antioxidant systems, which helped adjust ROS levels and prevent potential oxidative damage (Ferreira et al. 2018). As a consequence, photosynthetic stress was increased and more energy was lost *via* fluorescence dissipation, resulting in higher *Fo* and *Fm* values (Kulmann et al. 2022).

Conclusions

Differences in P level supply did not affect the initial growth of shoots and roots in clones of *E. saligna* and *E. urograndis*, which exhibited higher values of dry matter production, photosynthetic pigments, photosynthetic rate, and P accumulation in tissues, when compared to *E. dunnii.* Additionally, these clones showed lower stress and a reduced need to activate the antioxidant system. *Eucalyptus saligna* showed the highest rates of P influx and the lowest values of C_{min}, while *E. urograndis* had the lowest values of K_m under low P supply. *E. saligna* and *E. urograndis* were more efficient in absorbing phosphorous compared to *E. dunnii*, showing P uptake even at low concentrations. Biochemical and morpho-physiological parameters were positively correlated with uptake kinetic parameters, such as lower K_m and C_{min}, and could be usefully integrated in *Eucalyptus* selection and breeding programs.

The *Eucalyptus* clones used in the study are already established in the commercial plantations of the Company that provided rooted minicuttings. However, due to company restrictions, further details about the *Eucalyptus* clones cannot be specified.

Funding

The authors are grateful to the Council for Scientific and Technological Development (CNPq) of Brazil for the awarded grant, as well as to Federal University of Santa Maria, RS, Brazil for providing the space and equipment necessary for the conduction of the current study.

Authors' contributions

MVMA: Conceptualization, carrying out the experiments, biochemical and physiological analysis and data analysis, writing-revision and project administration. ÁLPB: Software, formal analysis, supervision and performance of experiments and biochemical and physiological analysis. CCK and TWP: Research, supervision, programming, carrying out experiments and biochemical and physiological analyses. MSSK: Formal Analysis, Software, Methodology, Supervision and Writing-Revision. DVV: Formal analysis and performance of the experiment and validation and project administration. TDA and VMS: validation, visualization, supervision, and analysis. GB: Fundraising, supervision, project co-supervision, writing and review. LAT: Conceptualization, project orientation, fundraising, biochemical and physiological analysis and writing-revision.

References

Aguilar MV, Sasso VM, Tabaldi LA (2023). *Handroanthus heptaphyllus* as bioindicator of chromium-contaminated environments. South African Journal of Botany 155: 35-44. - doi: 10.1016/j.sajb.2023.01.049

Alsherif EA, L-Shaikh A TM, Hamada A (2022). Heavy metal effects on biodiversity and stress responses of plants inhabiting contaminated soil in Khulais, Saudi Arabia. Biology 11: 01-21. - doi: 10.3390/biology11020164

Antunes E, Vuppaladadiyama AK, Kumar R, Vuppaladadiyam VSS, Sarmah A, Islam MA, Dada T (2022). A circular economy approach for phosphorus removal using algae biochar. Cleaner and Circular Bioeconomy 1: 1-9. - doi: 10.1016/j.clcb.2022.100005

Baligar VC, Fageria NK (2015). Nutrient use efficiency in plants: an overview. In: "Nutrient Use Efficiency: from Basics to Advances" (Rakshit A, Singh HB, Sen A eds), Springer, New Delhi, India, pp. 1-14. - doi: 10.1007/978-81-322-2169-2_1

Batista RO, Furtini Neto AE, Deccetti SFC, Viana CS (2016). Root morphology and nutrient uptake kinetics by Australian Cedar clones. Revista Caatinga 9: 153-162. - doi: 10.1590/1983-21252016v29n118rc

Beauchamp C, Fridovich I (1971). Superoxide dismutase: improved assays and an assay applicable to acrylamide gels. Analytical Biochemistry 8: 276-287. - doi: 10.1016/0003-2697(71)90370-8

Berghetti ALP, Araujo MM, Tabaldi LA, Turchetto F, Aimi SC, Rorato DG, Marchezan C, Griebeler AM, Barbosa FM, Brunetto G (2020). Morphological, physiological and biochemical traits of *Cordia trichotoma* under phosphorus application and a water-retaining polymer. Journal of Forestry Research 32: 855-865. - doi: 10.1007/s11676-020-01132-8

Bernardino KC, Pastina MM, Menezes CB, Sousa SM, Maciel LS, Carvalho Jr G, Guimarães CT, Magalhães JV (2019). The genetic architecture of phosphorus efficiency in sorghum involves pleiotropic QTL for root morphology and grain yield under low phosphorus availability in the soil. BMC Plant Biology 19 (1): 128. - doi: 10.1186/s12870-019-1689-y

Brunetto G, Rosa DJ, Ambrosini VG, Heinzen J, Ferreira PAA, Ceretta CA, Tiecher TL (2019). Use of phosphorus fertilization and mycorrhization as strategies for reducing copper toxicity in young grapevines. Scientia Horticulturae 248: 176-183. - doi: 10.1016/j.scienta.2019.01.026

Bulgarelli RG, Silva FMO, Bichara S, Andrade SAL, Mazzafera P (2019). Eucalypts and low phosphorus availability: between responsiveness and efficiency. Plant and Soil 445 (1-2): 349-368. - doi: 10.1007/s11104-019-04316-2

Chen Z, Khan A, Shia X, Hao X, Tan DKY, Luo H

(2020). Water-nutrient management enhances root morpho-physiological functioning, phosphorus absorption, transportation and utilization of cotton in arid region. Industrial Crops and Products 143: 111975. - doi: 10.1016/j.indcrop.2019.111975
Claassen N, Barber SA (1974). A method for characterizing the relation between nutrient concentration and flux into roots of intact plants. Plant Physiology 54: 564-568. - doi: 10.1104/pp.54.4.564
Del-Saz NF, Romero-Munar A, Cawthray GR, Palma F, Aroca R, Baraza E, Florez-Sarasa I, Lambers H, Ribas-Carbó M (2018). Phosphorus concentration coordinates a respiratory bypass, synthesis and exudation of citrate, and the expression of high-affinity phosphorus transporters in *Solanum lycopersicum*. Plant, Cell and Environment 41: 865-875. - doi: 10.1111/pce.13155
El-Moshaty FIB, Pike SM, Novacky AJ, Sehgal OP (1993). Lipid peroxidation and superoxide productions in cowpea (*Vigna unguicultata*) leaves infected with tobacco rings virus or southern bean mosaic virus. Journal Physiological and Molecular Plant Pathology 43: 109-119. - doi: 10.1006/pmpp.1993.1044
EMBRAPA (1999). Manual de análises químicas de solos, plantas e fertilizantes [Manual of chemical analysis of soils, plants and fertilizers]. Embrapa/CNPTIA, Brasília, Brazil, pp. 370. [in Portuguese]
Fernandes G, Marques ACR, Ribeiro BSMR, Cardoso PS, Tagliapietra EL, Friedrich ED, Weber PS, Krug AV, Kulmann MSS, Paula BV, Nicoloso FT, Brunetto G (2022). Potassium uptake kinetics in native forage grass species from Pampa Biome. Ciência Rural 52 (11): 155. - doi: 10.1590/0103-8478cr2020
Ferreira PAA, Tiecher T, Tiecher TL, Rangel WM, Soares CRFS, Ceretta CA (2018). Effects of *Rhizophagus clarus* and P availability in the tolerance and physiological response of *Mucuna cinereum* to copper. Plant Physiology Biochemistry 122: 46-56. - doi: 10.1016/j.plaphy.2017.11.006
Giannopolitis CN, Ries SK (1977). Purification and quantitative relationship with water-soluble protein in seedlings. Plant Physiology 48: 315-318. - doi: 10.1104/pp.59.2.315
Hernández I, Munné-Bosch S (2015). Linking phosphorus availability with photo-oxidative stress in plants. Journal of Experimental Botany 66: 2889-2900. - doi: 10.1093/jxb/erv056
Hiscox JD, Israelstam GF (1979). A method for the extraction of chlorophyll from leaf tissue without maceration. Canadian Journal of Botany 57: 1132-1334. - doi: 10.1139/b79-163
Irfan M, Aziz T, Maqsood MA, Bilal HM, Siddique KHM, Xu M (2020). Phosphorus (P) use efficiency in rice is linked to tissue-specific biomass and P allocation patterns. Scientific Reports 10: 1-14. - doi: 10.1038/s41598-020-61147-3
Janeeshma E, Johnson R, Amritha MS, Noble L, Aswathi KPR, Telesinski A, Puthur JT (2022). Modulations in chlorophyll *a* fluorescence based on intensity and spectral variations of light. International Journal of Molecular Sciences 23: 1-25. - doi: 10.3390/ijms23105599
Jin X, Zhu J, Wei X, Xiao Q, Xiao J, Jiang L, Xu D, Shen C, Liu J, He Z (2024). Adaptation strategies of seedling root response to nitrogen and phosphorus addition. Plants 13 (4): 536. - doi: 10.3390/plants13040536
Kassambara A, Mundt F (2017). Factoextra: extract and visualize the results of multivariate data analyses. CRAN Contributed Packages, version 1.0.7, website. - doi: 10.32614/CRAN.package.factoextra
Kulmann MSS, Eufrade-Junior HJ, Dick G, Schumacher MV, Azevedo GB, Guerra SPS (2022). Belowground biomass harvest influences biomass production, stock, export and nutrient use efficiency of second rotation Eucalyptus plantations. Biomass and Bioenergy 161: 106476. - doi: 10.1016/j.biombioe.2022.106476
Kulmann MSS, Paula BV, Sete PB, Arruda WS, Sans GA, Tarouco CP, Tabaldi LA, Nicoloso FT, Brunetto G (2020). Morphological and kinetic parameters of the absorption of nitrogen forms for selection of *Eucalyptus* clones. Journal of Forestry Research 32: 1599-1611. - doi: 10.1007/s11676-020-01195-7
Kulmann MSS, Arruda WS, Vitto BB, Souza ROS, Berghetti ALP, Schumacher MV, Brunetto G (2021). Morphological and physiological parameters influence the use efficiency of nitrogen and phosphorus by *Eucalyptus* seedlings. New Forests 53 (3): 431-448. - doi: 10.1007/s11056-021-09864-z
Li P, Weng J, Rehman A, Niu Q (2022). Root morphological and physiological adaptations to low phosphate enhance phosphorus efficiency at melon (*Cucumis melo* L.) seedling stage. Horticulturae 8 (7): 636. - doi: 10.3390/horticulturae8070636
Lima MB, Cappa EP, Silva-Junior OB, Garcia C, Mansfield SD, Grattapaglia D (2019). Quantitative genetic parameters for growth and wood properties in *Eucalyptus "urograndis"* hybrid using near-infrared phenotyping and genome-wide SNP-based relationships. Plos One 14: 0218747. - doi: 10.1371/journal.pone.0218747
Liu D (2021). Root developmental responses to phosphorus nutrition. Journal of Integrative Plant Biology 63: 1065-1090. - doi: 10.1111/jipb.13090
Loreto F, Velikova V (2001). Isoprene produced by leaves protects the photosynthetic apparatus against ozone damage, quenches ozone products, and reduces lipid peroxidation of cellular membranes. Plant Physiology 12: 1781-1787. - doi: 10.1104/pp.010497
Manca A, Silva MR, Guerrini IA, Fernandes DM, Bôas RLV, Capra GF (2020). Composted sewage sludge with sugarcane bagasse as a commercial substrate for Eucalyptus urograndis seedling production. Journal of Cleaner Production 269 (Suppl. 1): 122145. - doi: 10.1016/j.jclepro.2020.122145
Martinez HE, Olivos A, Brown PH, Clemente JM, Bruckner CH, Jifon JL (2015). Short-term water stress affecting NO_3^- absorption by almond plants. Scientia Horticulturae 197: 50-56. - doi: 10.1016/j.scienta.2015.10.040
Meng X, Chen W, Wang Y, Huang Z, Chen L, Yang L (2021). Effects of phosphorus deficiency on the absorption of mineral nutrients, photosynthetic system performance and antioxidant metabolism in *Citrus grandis*. Plos One 16: e0246944. - doi: 10.1371/journal.pone.0246944
Mittler R, Zandalinas SI, Fichman Y, Van Breusegem F (2022). Reactive oxygen species signalling in plant stress responses. Nature Reviews Molecular Cell Biology 23: 663-679. - doi: 10.1038/s41580-022-00499-2
Murphy J, Riley JPA (1962). Modified single solution method for determination of phosphate in natural waters. Analytica Chimica Acta 27: 31-36. - doi: 10.1016/S0003-2670(00)88444-5
Nielsen NE, Barber SA (1978). Differences among genotypes of corn in the kinetics of P uptake. Agronomy Journal 70: 695-698. - doi: 10.2134/agronj1978.00021962007000050001xa
Paula BV, Marques ACR, Rodrigues LAT, Souza ROS, Kulmann MSS, Brunetto G (2018). Morphological and kinetic parameters of the uptake of nitrogen forms in clonal peach rootstocks. Scientia Horticulturae 239: 205-209. - doi: 10.1016/j.scienta.2018.05.038
Paula BV, Sete PB, Berghetti ALP, Silva LOS, Jung JP, Nicoloso FT, Brunetto G (2022). Kinetic parameters related to nitrogen uptake in Okinawa peach rootstocks are altered by scion Chimarrita. Journal of the Science of Food and Agriculture 103 (2): 917-923. - doi: 10.1002/jsfa.12203
Pereira FCM, Tayengwa R, Alves PLCA, Peer WA (2019). Phosphate status affects phosphate transporter expression and glyphosate uptake and transport in grand eucalyptus (*Eucalyptus grandis*). Weed Science 67: 29-40. - doi: 10.1017/wsc.2018.58
Pinto SIC, Neto AEF, Moretti BS, Santos CF, Andrade AB, Guelfi D (2020). Root morphology and joint uptake kinetics of phosphorus, potassium, calcium and magnesium in six eucalyptus clones. Communications in Soil Science and Plant Analysis 52: 45-57. - doi: 10.1080/00103624.2020.1845358
R Core Team (2019). R: a language and environment for statistical computing. R Foundation for Statistical Computing, Vienna, Austria. [online] URL: http://www.r-project.org/
Scanavacca Júnior L, Garcia JN (2021). Water storage in *Eucalyptus urophylla* progenies. Scientia Forestalis 49 (132): e3715. - doi: 10.18671/scifor.v49n132.10
Siddiqi MY, Glass ADM (1981). Utilization index: a modified approach to the estimation and comparison of nutrient utilization efficiency in plants. Journal of Plant Nutrition 4: 289-302. - doi: 10.1080/01904168109362919
Silva LOS, Schwalbert R, Schwalbert R, Tassinari A, Garlet L, De Conti L, Ciotta M, Brunetto G (2023). Phosphorus critical levels in soil and grapevine leaves for South Brazil vineyards: a Bayesian approach. European Journal of Agronomy 144: 126752. - doi: 10.1016/j.eja.2023.126752
Tabaldi LA, Ruppenthal R, Cargnelutti Morsch VM, Pereira LB, Schetinger MRC (2007). Effects of metal elements on acid phosphatase activity in cucumber (*Cucumis sativus* L.) seedlings. Environmental and Experimental Botany 59: 43-48. - doi: 10.1016/j.envexpbot.2005.10.009
Teng W, Zhao Y, Zhao X, He X, Ma W, Deng Y, Chen X, Tong Y (2017). Genome-wide identification, characterization, and expression analysis of PHT1 phosphate transporters in wheat. Frontiers in Plant Science 8 (e13548): 798. - doi: 10.3389/fpls.2017.00543
Wang J, Chen Y, Wang P, Li YS, Wang G, Liu P, Khan A (2018). Leaf gas exchange, phosphorus uptake, growth and yield responses of cotton

cultivars to different phosphorus rates. Photosynthetica 56 (4): 1414-1421. - doi: 10.1007/s11099-018-0845-1
Yang M, Wang C, Hassan MA, Li F, Xia X, Shi S, Xiao Y, He Z (2021). QTL mapping of root traits in wheat under different phosphorus levels using hydroponic culture. BMC Genomics 22 (1): 224. - doi: 10.1186/s12864-021-07425-4
Zeraik AE, Souza FS, Fatibello-Filho O (2008). Desenvolvimento de um spot test para o monitoramento da atividade da peroxidase em um procedimento de purificação [Development of a spot test for monitoring peroxidase activity in a purification procedure]. Química Nova 31: 31-734. [in Portuguese]
Zheng C, Wang Y, Yang D, Xiao S, Sun Y, Huang J, Peng S, Wang F (2022). Biomass, radiation use efficiency, and nitrogen utilization of ratoon rice respond to nitrogen management in Central China. Frontiers in Plant Science 13: 536. - doi: 10.3389/fpls.2022.889542

Supplementary Material

Fig. S1 - Mean values recorded for root length, root surface area, root volume and average root diameter in the *Eucalyptus* clones.

Fig. S2 - Mean values recorded for net photosynthetic rate (A), transpiration rate (E), intercellular CO_2 concentration (Ci), water use efficiency (WUE) in the *Eucalyptus* clones.

Fig. S3 - Mean values recorded for superoxide dismutase activity in shoots (Shoot SOD) and roots (Root SOD), guaiacol peroxidase activity in shoots (Shoot POD) and roots (Root POD), and acid phosphatase activity in shoots (Shoot Apase) and roots (Root APase) in the *Eucalyptus* clones.

Fig. S4 - Mean values recorded for P absorption efficiency (PAE), P use efficiency in roots (Root PUE), P use efficiency in shoots (Shoot PUE), Total P use efficiency (Total PUE) in the *Eucalyptus* clones.

Link: Miranda_4643@suppl001.pdf